Supplementary Information

The effects of edge-enhanced filter on increasing LGN visibility are shown for all RPE65 patients (Figure S1) and seven of the sighted control (Figure S2) participants. Column A is the unfiltered original raw images from the right LGN in the coronal orientation of all participants. The same slices undergone edge enhancement algorithm are presented in Column B. The comparison between the columns A and B clearly showing the increased visibility of LGN and the efficacy of the edge enhancement algorithm. Column C represents the delineated LGN in the same representative edge enhance slice in the coronal orientation.

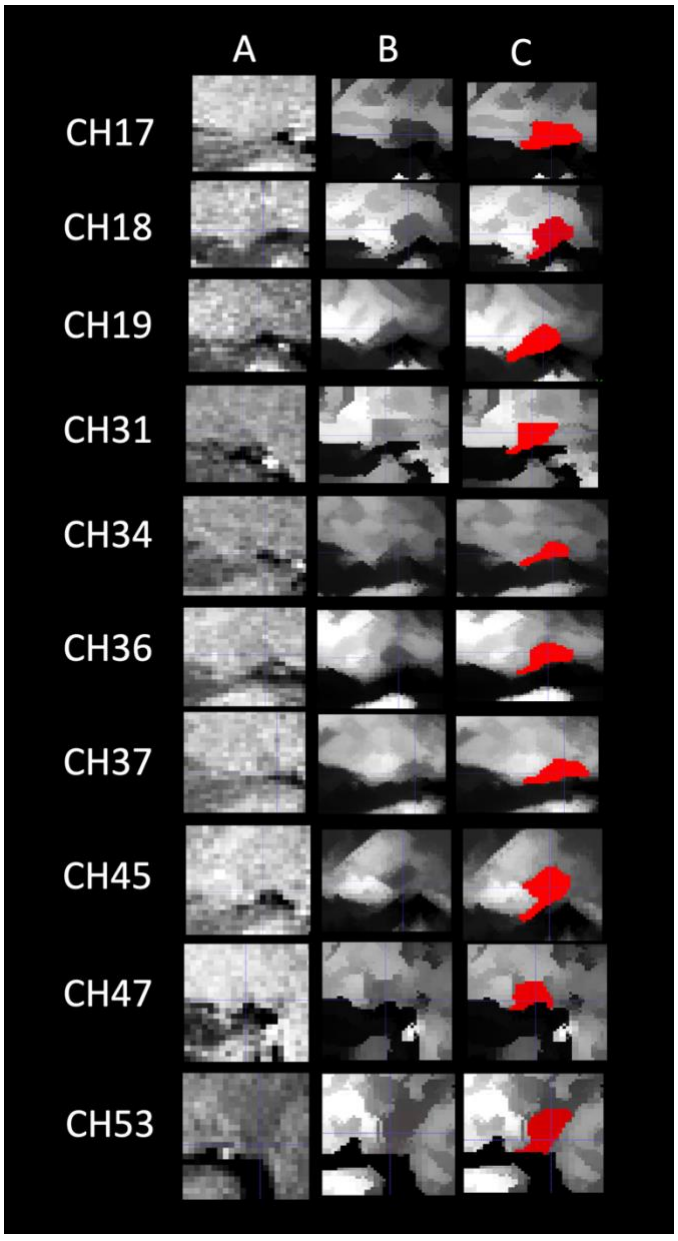

Figure S1: Comparison of the raw and filtered images of a representative slice in coronal orientation for all RPE65 patients.

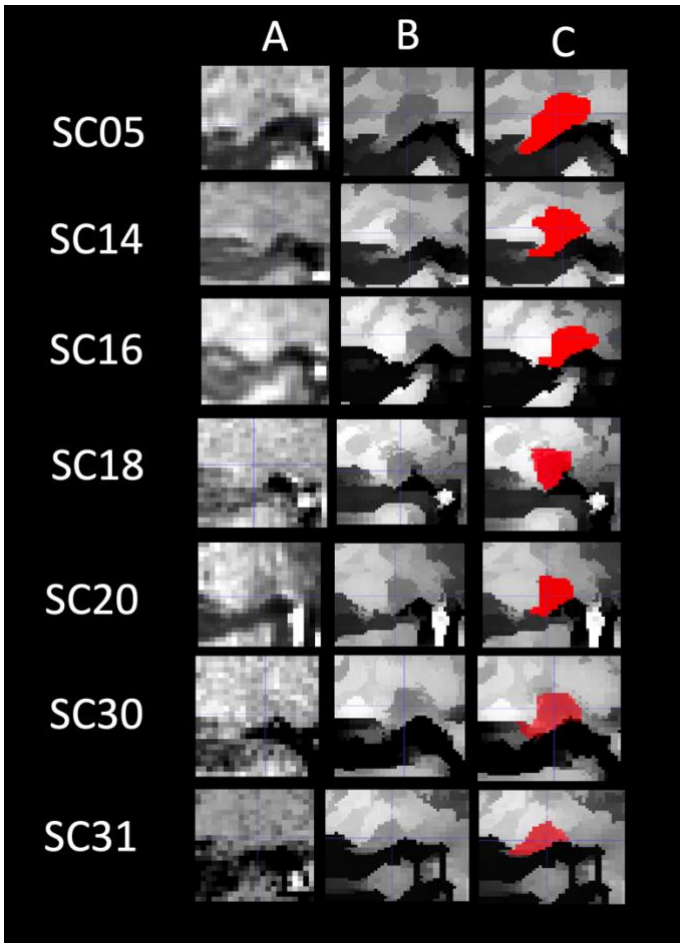

Figure S2: Comparison of the raw and filtered images of a representative slice in coronal orientation for seven sighted controls.

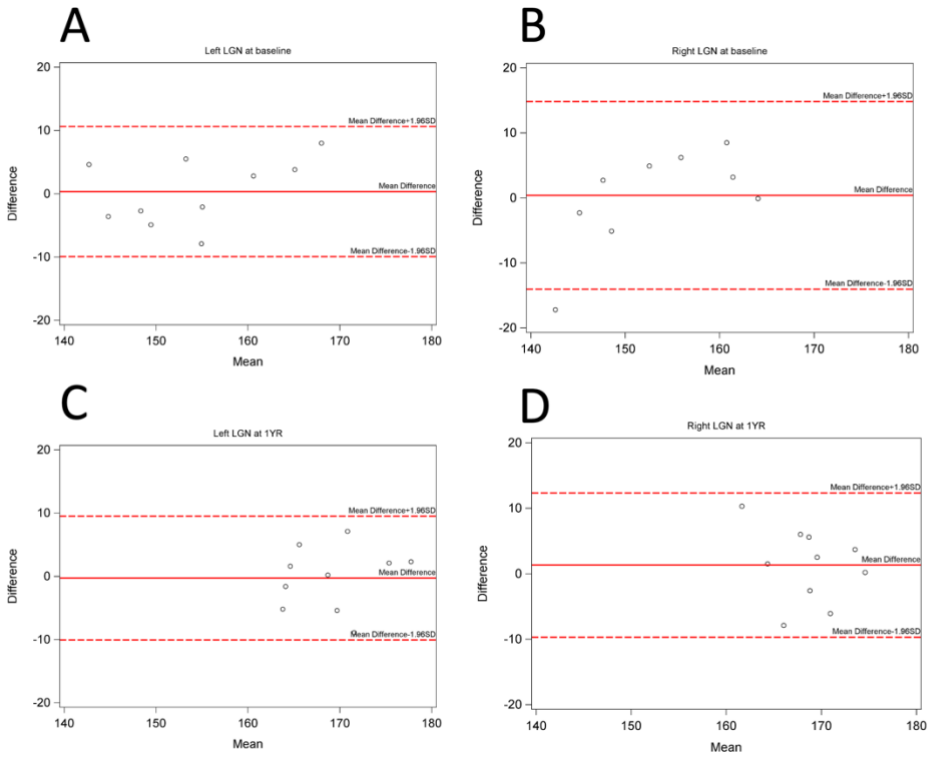

Figure S3: The inter-rater variability Bland-Altman plots for the left and right LGN volume measures at baseline and 1 YR. **(A)**: The difference in the left LGN volume measurements between the two raters were well within ±10 mm^3 at baseline for the left LGN volume measures. **(B):** Similar to the left LGN, the measurements from the two raters were within ±10 mm^3 of the mean difference except for one participant. **(C):** The differences in the left LGN measures of the RPE65 patients between the two raters one year after bilateral retinal intervention. **(D):** The differences in the right LGN measures of the RPE65 patients between the two raters one year after bilateral retinal intervention. The statistical assessment for the inter-rater reliability is presented in Table 2 of the main manuscript.